

# The Light–Cone nonperturbative dynamics of meson wave functions

V.L. Morgunov, V.I. Shevchenko, Yu.A. Simonov

*Institute for Theoretical and Experimental Physics*

*RU-117259, Moscow, Russia*

(May 13, 2019)

The light–cone Hamiltonian, incorporating the nonperturbative dynamics of the  $q\bar{q}$  system connected by the string is solved numerically. The spectrum is shown to coincide with that of the center–of–mass Hamiltonian within the accuracy of computation, displaying the expected degeneracies of the string states, but an overall shift due to different treatment of Z–graphs is obtained. The nonperturbative wave functions are calculated directly from the light–cone Hamiltonian for the first time, thus allowing the explicit estimation of nonperturbative effects in the parton model language. In this way one obtains the string contribution to the parton distributions and in the formfactors and structure functions.

## I. INTRODUCTION

The light–cone description of the hadron wave functions is widely used, since it allows to get a direct connection to the parton model and its QCD improvements [1]. The latter however are mostly perturbative and nonperturbative contributions are introduced via OPE and QCD sum–rules. In this way the concept of the string – the main nonperturbative QCD phenomenon – is totally lost. On physical grounds it seems that the string is the essential ingredient of the dynamics for large ( $r \geq 0.5 fm$ ) distances, and it would be interesting to understand its contribution to the light–cone wave functions, formfactors, structure functions etc.

In particular, what is the QCD string in the parton language? Should one associate it with the gluon contribution as an assembly of gluons compressed inside the string – or with the constituent quark mass?

There two contrasting points of view have been proposed already decades ago [2,3]. In [2] the sea quarks and gluons enter as separate entities and one could associate the gluon distribution with the string in the same way as photons with the Coulomb field of the charge in the Williams–Weizsäcker method. In contrast to that in [3] the quarks have been considered as constituents with structure, and string does not appear separately. Recently a quantitative analysis was performed [4] of quark distribution in the pion starting from that in the nucleon and assuming the same internal structure of quarks in nucleon and in pion. It is still an open question how the structure of the constituent quarks is formed, and to which extent it can be explained by the adjacent piece

of the string. This problem can be elucidated partly in the present approach, since our light–cone Hamiltonian contains the string on the light cone explicitly. It allows to separate the contribution of the string to the parton distribution, in particular to the momentum sum–rule. There is another source of structure in the constituent quark – chiral symmetry breaking which creates the chiral mass of quark. This problem will not be discussed below, see e.g. [5].

There are many other questions which can be asked from a decent light–cone Hamiltonian, incorporating  $q\bar{q}$  system with the proper light–cone nonperturbative dynamics. An important advantage of the light–cone wave functions is that they allow to calculate formfactors and structure functions directly, without additional boosts, which typically are the dynamical ones, i.e. require the use of the Hamiltonian.

Another point to clarify is the comparison of the proper light–cone dynamics incorporated in the wave–function of the light–cone Hamiltonian [6] with the popular ansatz where one is simply using the c.m. wave function expressing it through the light–cone variables [7].

But the first question to answer is the comparison of the c.m. and light–cone spectra. In the c.m. system the Hamiltonian of the spinless  $q\bar{q}$  system, connected by the minimal (i.e. without vibrations) string was obtained in [8]. The backward–in–time motion or so called Z–graphs are suppressed there because Z–graphs contains backward moving string and the corresponding increase in the action damps the amplitude. On the light–cone Z–graphs are treated differently and do not appear in lowest orders of perturbation theory and comparing spectrum with that of c.m. one can visualize the difference due to the different contribution of Z–graphs.

Another typical feature of the light–cone Hamiltonian should be mentioned. As we shall see in Section 2 the form found in [6] explicitly contains the z–axis component of the angular momentum,  $L_z$  which is not Lorenz–invariant and hence the light–cone spectrum should demonstrate degeneracy for different values of  $L_z$  with the same  $L^2$ . This degeneracy will be explicitly demonstrated below. Therefore all states of the system including angular excitations may be calculated using the Hamiltonian with  $L_z = 0$ . It is known (see [8] and also [9]) that the problem under consideration possesses the dynamical symmetry which implies that quasiclassical frequencies of the radial and orbital motions are approximately proportional to each other with the coefficient

2. Thus the light–cone Hamiltonian should also manifest this dynamical symmetry.

The plan of the paper is as follows. In Section 2 we start with the light–cone Hamiltonian in 3+1–dimensions from [6] and prepare it for numerical computations. As in [6], we simplify the matter considerably, neglecting spins, perturbative gluon exchanges and additional quark pairs. The first two points are unessential at large distances, which are of the main interest for us here but seriously contribute to the lowest mass mesons. We plan to include these effects in next publications. Sea quarks are expected to contribute some 10% effect and disappear in the large  $N_c$  limit. As it is, we are confined to the valence quark sector of the Fock column wave function.

In Section 3 general properties of solutions and the physical meaning of parameters  $\mu_i, x$  and  $\rho$  are discussed. We also demonstrate the limiting procedure reducing the 3+1 Hamiltonian to the 1+1 problem, following the method of [6] and compare properties of 3+1 and 1+1 solutions. In Section 4 the formfactors and structure functions are defined through the solutions of the light–cone Hamiltonian and physical limiting cases are discussed. In Section 5 the numerical procedure used for the solution of the eigenvalue equation is explained. In Section 6 we present numerical results and discuss them from different points of view, e.g. comparing center–of–mass spectrum and wave functions with those of the light–cone. Special attention is paid to the procedure used in literature [7] where the c.m. wave function is kinematical expressed in terms of the light–cone variables. A short conclusion and perspectives are given in Section 7. Two appendices, A and B serve to illustrate the derivation of the Hamiltonian (1) and the final form of equation (13) to be solved numerically.

## II. THE GREEN'S FUNCTION AND THE HAMILTONIAN

We consider the relativistic quark–antiquark pair with the masses  $m_1$  and  $m_2$  connected by the straight–line Nambu–Goto string with the string tension  $\sigma$  in 3+1 dimensional space–time, see [6] and Appendix A of the present paper for details. We start from the expression for the classical light–cone Hamiltonian function in 3+1 dimensions

$$H = \frac{1}{2} \left\{ \frac{m_1^2}{\mu_1} + \frac{m_2^2}{\mu_2} + \frac{L_z^2}{a r_\perp^2} + \frac{(p_\perp r_\perp + \gamma r_-)^2}{\tilde{\mu} r_\perp^2} + \int \frac{\sigma^2}{\nu} d\beta r_\perp^2 + \frac{\nu_0 P_+}{\mu_1 + \mu_2} \frac{r_-^2}{r_\perp^2} \right\} \quad (1)$$

In Appendix A we briefly derive this expression, using [6] and omitting unessential details. Here  $\mu_1, \mu_2$  are einbein fields, playing the role of  $P_+$  momenta of the particles,  $\tilde{\mu} = \mu_1 \mu_2 / (\mu_1 + \mu_2)$ ,  $\nu_0 = \int_0^1 d\beta \nu(\beta)$  and  $\nu(\beta)$  is the einbein field with the physical meaning of the

$P_+$ –momentum, carried by the string. As it has been mentioned above, the Hamiltonian explicitly depends on  $L_z^2 = \vec{p}_\perp^2 \vec{r}_\perp^2 - (\vec{p}_\perp \vec{r}_\perp)^2$ , the corresponding mass parameter in the denominator in (1) is equal to

$$a = \mu_1(1-x)^2 + \mu_2 x^2 + \int_0^1 d\beta \nu(\beta) (\beta-x)^2 \quad (2)$$

The variable  $x$  in the above expression is defined as (see Appendix A for details):

$$x = \frac{\mu_1 + \langle \beta \rangle \nu_0}{P_+} \quad (3)$$

where

$$P_+ = \mu_1 + \mu_2 + \nu_0 \quad (4)$$

is the light–cone total momentum of the system. Also

$$\gamma = \nu_0 \left( \langle \beta \rangle - \frac{\mu_1}{\mu_1 + \mu_2} \right) \quad (5)$$

where  $\langle \beta \rangle = \int_0^1 d\beta \beta \nu(\beta) / \int_0^1 d\beta \nu(\beta)$ .

The corresponding Green's function is defined as an integral over the dynamical fields as well as over the einbein fields:

$$G(x\bar{x}; y\bar{y}) = \int D\mu_1 D\mu_2 D\nu DR_\mu Dr_\mu e^{-A} \quad (6)$$

where  $A$  is the euclidean action. Separating out the center of mass motion one defines the Hamiltonian from the corresponding Minkowskian action  $A^M$ :

$$A^M = \int dz_+ L^M, \quad H = p_\perp \dot{r}_\perp - L^M \quad (7)$$

with  $p_\perp = \partial L^M / \partial \dot{r}_\perp$ . This is the light–cone Hamiltonian of our problem (1).

As the next step one should quantize the classical Hamiltonian function. Before doing it, one should choose the appropriate set of dynamical variables. Three einbein fields  $\mu_1, \mu_2, \nu$  introduced above play different dynamical roles. In the nonrelativistic case  $m_1, m_2 \gg \sqrt{\sigma}$  (and therefore for the free particles) the dependence of Hamiltonian (and wave functions) on  $\nu$  can be correctly found by minimization procedure with  $\nu$  taken as a classical variable. This is in its turn a consequence of the fact, that string in our approach is the minimal one – it has no internal degrees of freedom and may only stretch or rotate as a whole.

On another hand,  $\mu_1$  and  $\mu_2$  on the light cone play the role of legitimate quantum dynamical degrees of freedom and can be expressed through  $x$  and  $P_+$  as in (4) and (3).

There are two canonically conjugated pairs  $\{\vec{p}_\perp, \vec{r}_\perp\}$  and  $\{x, (P_+ r_-)\}$  (see Appendix A). We introduce also a new dimensionless variable  $\tilde{y}$  instead of  $\nu$ :  $\tilde{y}(\beta) = \nu(\beta) / P_+$ . It satisfies the obvious condition:  $0 < \tilde{y} < 1$ .

This variable depends on  $\vec{r}_\perp$  as well as on  $(P_+ r_-)$ . Rigorously speaking one should extract this dependence by the minimization of the Hamiltonian with respect to  $\tilde{y}$  as it has been explained above. Instead an easier (however approximate) way is chosen. On physical grounds it can be shown that for small  $r_\perp^2$  one has  $\tilde{y}_0 = \int_0^1 \tilde{y} d\beta \sim \text{const} \cdot r_\perp^2$  so that linear string energy density  $\tilde{y}_0/r_\perp^2$  stays finite if  $r_\perp^2 \rightarrow 0$ , and using this property one can reproduce the correct 1+1 limit, namely 't Hooft equation [10], from the 3+1 light-cone Hamiltonian (1) (see [6] and the next section). On the other hand, if distances are increasing,  $\tilde{y}_0$  tends to some limiting value which is determined by the virial theorem arguments. So one can parameterize  $\tilde{y}$  introducing several parameters and replace the minimization in the functional sense by the ordinary minimization with respect to these parameters. We have chosen the simplest 2-parametric form for  $\tilde{y}$ :

$$\tilde{y} = \frac{yt}{1 + \alpha t} \quad (8)$$

where  $t = r_\perp^2$  and  $y$  and  $\alpha$  are free parameters. The requirement  $0 < \tilde{y} < 1$  leads to the restriction  $0 < y < \alpha$ . Let us stress again that this parameterization is the matter of convenience and all physical results are determined from the requirement that every energy level should have its own minimum.

It is easy to see from (3), that the  $x$ -variable is the part of the total momentum, carried by the first quark itself and a part of the string, "belonging" to this quark. Rewriting (3) in the form:

$$\frac{\mu_1}{P_+} = x - \tilde{y} \langle \beta \rangle ; \quad \frac{\mu_2}{P_+} = (1 - x) - \tilde{y}(1 - \langle \beta \rangle) \quad (9)$$

one can conclude, that for the given  $\tilde{y}$  the variable  $x$  may vary in the following limits:

$$\tilde{y} \langle \beta \rangle \leq x \leq 1 - \tilde{y}(1 - \langle \beta \rangle) \quad (10)$$

It is more convenient to make rescaling to a new variable  $\rho$  which varies from zero to unity:

$$x = \tilde{y} \langle \beta \rangle + (1 - \tilde{y})\rho ; \quad 0 \leq \rho \leq 1 \quad (11)$$

The quantity we are really interested in is the mass operator squared:

$$\hat{M}^2 = 2 \hat{H} P_+ \quad (12)$$

and for  $\hat{M}^2$  we have the Schrödinger equation of the following form:

$$A_1 \psi'' + A_2 \ddot{\psi} + A_3 \dot{\psi}' + A_4 \psi' + A_5 \dot{\psi} + A_6 \psi = M^2 \psi \quad (13)$$

here  $\psi = \psi(\rho, \vec{r}_\perp)$  and two independent variables are  $\rho \in [0, 1]$  and  $t = r_\perp^2 \in [0, \infty)$ ;  $\psi' \equiv \partial\psi/\partial t$ ;  $\dot{\psi} \equiv \partial\psi/\partial\rho$ ; the coefficients  $A_i$  depend on  $\rho$  and  $t$ . The derivation

of (13) from the Hamiltonian (1) as well as the explicit form of the functions  $A_i$  may be found in Appendix B. The following boundary conditions are to be imposed:

$$\psi(0, t) = \psi(1, t) = 0 \quad , \quad \psi(\rho, t \rightarrow \infty) = 0 \quad (14)$$

with the normalization of the solution:

$$\int_0^1 d\rho \int d^2 r_\perp |\psi(\rho, \vec{r}_\perp)|^2 = 1 \quad (15)$$

We discuss properties of solutions of (13) in the next section.

### III. GENERAL PROPERTIES OF THE SOLUTIONS.

In this section we shall discuss the physical meaning of our variables  $x, \mu, \rho$  and  $\tilde{y}$  and some properties of the solution  $\psi(\rho, t)$ . Rewriting (4) as

$$1 = \frac{\mu_1}{P_+} + \frac{\mu_2}{P_+} + \tilde{y} \quad (16)$$

one can conclude that  $\mu_i/P_+$  and  $\tilde{y}$  have the meaning of the parts of the total momenta  $P_+$ , associated with the  $i$ -th quark and string respectively. This identification is also supported by the form of the Hamiltonian (1), where masses enter as  $m_i^2/2\mu_i$  so that in the infinite-momentum frame it becomes  $m_i^2/2p_+^i$ . The similar situation occurs in the c.m. system where  $\mu_i$  and  $\nu$  have the meaning of the energy, associated with the quarks and the string. One notes the essential difference in the way these einbein fields are treated in the c.m. Hamiltonian and on the light-cone. In the former case  $\mu_i$  enter on the same grounds as  $\nu$  (or  $\tilde{y}$ ) and are to be found by minimization of the Hamiltonian. In contrast to that on the light-cone  $\mu_1, \mu_2$  are expressed through  $\tilde{y}$  and  $x$  as in (3) and  $x$  is the canonical momentum, conjugated to the coordinate  $P_+ r_-$  ( see Appendix A), namely:

$$[x, P_+ r_-] = -i \quad (17)$$

Hence  $\mu_i$  are promoted to be quantum operators with average values to be found from the solution of the "Schrödinger equation" (13) Without the string, when  $\tilde{y} = 0$  one has  $\mu_1 = xP_+$  ;  $\mu_2 = (1 - x)P_+$  and the correspondence with the naive parton model is trivial. However when  $\tilde{y} \neq 0$  there are no *a priori* reasons to associate our  $x$  with the Feynman  $x$  parameter, but instead one could call  $\mu_i/P_+$  the Feynman  $x$  parameter and associate  $\tilde{y}$  with the Feynman parameter for the string.

However the strong interaction between the string and quarks taken into account in the light-cone Hamiltonian (1) invalidates the literal interpretation of our results in the free parton language – one can only interpret the averaged values of  $\mu_1, \mu_2$  together with the minimized value for  $\tilde{y}$ .

Then one can consider the momentum sum–rules for the quark structure functions  $f_2^F(x_F)$  where the quark Feynman parameter  $x_F$  normalized to the interval  $[0,1]$  should be associated with the parameter  $\rho$  from (11) which is connected with  $\mu_i$  as follows:

$$\frac{\mu_1}{P_+} = (1 - \tilde{y})\rho ; \quad \frac{\mu_2}{P_+} = (1 - \tilde{y})(1 - \rho) \quad (18)$$

Therefore as we shall discuss later the average momentum carried by the quarks is equal to  $(1 - \tilde{y})$  while the rest,  $\tilde{y}$  is carried by gluons assembled into the string – nonperturbative gluons. This interpretation of the missing momentum (around one half in experiment [1] ) as due to the string was suggested already in [2]. Now we are in the position to calculate this quantity and compare to the experiment which we shall do in Section 6. As we shall see, the main missing ingredient in our Hamiltonian and wave functions is the sea quarks and "sea gluons" – i.e. gluons which excite the string and make it vibrating instead of keeping the straight–line form we have considered. From this point of view our wave function, the solution of (13) is the first upper entry in the Fock column, containing states with 1,2,... gluons, "sitting on the string" and exciting it to the first, second, etc. vibrating string state. It is the whole Fock column which is responsible for the Regge behaviour of cross–sections and Regge asymptotic of structure functions near  $\rho \rightarrow 0$ . In this paper we concentrate on the properties of the sector with two valence quarks and minimal (i.e. nonvibrating) string, leaving the general discussion of the QCD reggeons and the pomeron to a future publication.

Let us now turn to the properties of the wave functions and, in particular, their behaviour at the boundaries. Inserting in (13)  $\psi(\rho) \sim \rho^\alpha$  and  $(1 - \rho)^\alpha$  near the points  $\rho = 0$  and 1 respectively one obtains the only solution  $\alpha = 1$  at all  $t$  hence the boundary conditions (14) are satisfied. Similarly, representing  $\psi(\rho, t = r_\perp^2)$  at large  $t$  in the form

$$\psi(\rho, t) \sim A(\rho) \exp(-\gamma(\rho)t^\xi) \quad (19)$$

yields  $\xi = 1$  and some complicated equation for  $\gamma(\rho)$ .

Finally, we discuss in this section the limit of the (1+1) 't Hooft equation [10]. Following the arguments given in [6] we look for the limit  $t \rightarrow 0$  with  $\tilde{y} = yt/(1 + \alpha t) \rightarrow 0$  and  $y$  fixed and to be found from the minimization. As a result, one obtains:

$$H_1 = \frac{1}{2} \left\{ \frac{m_1^2}{\mu_1} + \frac{m_2^2}{\mu_2} + \int \frac{\sigma^2}{y(\beta)} d\beta + \int y(\beta) d\beta \frac{P_+ r_-^2}{\mu_1 + \mu_2} \right\} \quad (20)$$

Note that the string part in the sum (16) disappears because of  $\tilde{y} = 0$  but  $y$  is nonzero and ensures the string–like potential dynamics. Taking the extremum of (20) with respect to  $y(\beta)$  and introducing  $x$  instead of  $\mu_1, \mu_2$  where  $\mu_1 = P_+ x, \mu_2 = P_+(1 - x)$  one obtains:

$$M^2 = 2P_+ H_1 = \frac{m_1^2}{x} + \frac{m_2^2}{1-x} + 2\sigma |P_+ r_-| \quad (21)$$

From (21) one easily deduces the 't Hooft equation [10]:

$$\left( \frac{m_1^2}{x} + \frac{m_2^2}{1-x} \right) \psi(x) - \frac{\sigma}{2\pi} \int \frac{dy \psi(y)}{(x-y)^2} = M^2 \psi(x) \quad (22)$$

Thus the 't Hooft solutions [10] which approximately are:

$$\psi_n(x) = C_n \sin \pi n x \quad (23)$$

can be thought of as limiting case  $t \rightarrow 0$  of our solutions but one should have in mind that the extremum value of  $y$  leading to the 't Hooft equation (22) in general does not coincide with the extremum value in our equation (13) obtained for all nonzero  $t$ . Still the behaviour at the boundary points  $x = 0, 1$  ( $\rho = 0, 1$  in our case) and the general pattern of our solution  $\psi(\rho, t = 0)$  is closely resembling those of 't Hooft solutions.

#### IV. FORMFACTORS AND STRUCTURE FUNCTIONS

The formfactor of the bound system of two spinless quarks can be expressed through the wave–function in the momentum representation, depending on  $x$  and on the relative momentum  $p_\perp$  as follows (for equal mass quarks) [11]:

$$F(q^2) = \int \psi(x, \vec{k}_\perp) \psi^*(x, \vec{k}_\perp + (1-x)\vec{q}_\perp) dx d^2 k_\perp \quad (24)$$

Our wave function is defined in the mixed space  $\rho, r_\perp^2 = t$  hence one obtains:

$$F(q^2) = \pi \int_0^1 \int_0^1 |\psi(\rho, t)|^2 J_0 \left\{ q\sqrt{t} \left[ 1 - \rho + \tilde{y}(\rho - \frac{1}{2}) \right] \right\} d\rho dt \quad (25)$$

where we have exploited relation (11) with  $\langle \beta \rangle = 1/2$ . For  $q^2 = 0$  the usual normalization follows  $F(0) = 1$  since our wave function is normalized as

$$\pi \int_0^1 \int_0^1 |\psi(\rho, t)|^2 d\rho dt = 1 \quad (26)$$

Note that the effect of the electromagnetic current, which interacts only with the charged quark (and anti-quark) and does not interact directly with the string, enters (25) through the factor  $(1-x)\vec{q} = [1 - \rho + \tilde{y}(\rho - 1/2)]\vec{q}$ , and not through  $\mu$  or  $\rho$ . This is the result of the fact, that the parameter  $x$  governs the distribution of the momentum between the center of mass and relative coordinates  $\vec{R}_\perp$  and  $\vec{r}_\perp$ .

Let us notice, that because we neglect perturbative gluon exchanges, our formfactor does not have the familiar quark asymptotic  $F(q^2) \sim \text{const}/q^2$  for  $q^2 \rightarrow \infty$ , but rather corresponds to the nonperturbative part which is believed to dominate the low- $q$  region (actually the experimentally accessible region of today) [12].

From (25) and the behaviour of  $\psi(\rho, t)$  at large  $t$  and  $\rho \rightarrow 1$ , equation (19), one easily obtains that

$$F(q^2) \sim \frac{\text{const}}{|q|^3}, \quad |q| \rightarrow \infty \quad (27)$$

We turn now to the structure function (or quark distribution function). As well as in case of the formfactor, since as it is produced by the external current it is natural to define it a function of  $x$ , but to compare it with standard results normalized to the interval  $[0,1]$ , we choose to define it as a function of  $\rho$ .

Thus, the parton distribution inside our meson wave function can be written as:

$$q(\rho) = \pi \int_0^\infty |\psi(\rho, t)|^2 dt \quad (28)$$

and the normalization of  $q(\rho)$  due to (26) is

$$\int_0^1 q(\rho) d\rho = 1. \quad (29)$$

The momentum sum-rule, using (16) and (18) is (for equal masses of quark and antiquark)

$$2 \int_0^1 q(\rho) \rho (1 - \langle \tilde{y} \rangle) d\rho + \int_0^1 q(\rho) \langle \tilde{y} \rangle d\rho = 1 \quad (30)$$

where  $\langle \tilde{y} \rangle$  is obtained by integration with  $|\psi(\rho, t)|^2$ ,

$$\langle \tilde{y} \rangle = \pi \int_0^\infty \int_0^1 \tilde{y} |\psi(\rho, t)|^2 d\rho dt \quad (31)$$

Comparing with the standard energy-momentum sum-rule [1] containing the gluon distribution  $g(x)$ , one may associate it with  $\tilde{y}$  as follows  $\int_0^1 g(x) x dx \Rightarrow \langle \tilde{y} \rangle$ .

From (30, 10) one can see that both valence quarks together carry the part of momentum  $P_+$  equal to  $1 - \langle \tilde{y} \rangle$ , while the string carries on average  $\langle \tilde{y} \rangle P_+$ .

The essential difference of the minimal string from the gluon distribution  $g(x)$  is that the former is fixed in the quasiclassical einbein formalism and has no dispersion – unlike free gluons which can carry any part of the total momentum  $P_+$ .

Let us discuss finally the correspondence between  $q(\rho)$  and  $F(q^2)$  (the Drell-Yan-West duality [13]). If  $F(q^2)$  behaves as  $(q^2)^{-n}$  at large  $q^2$ , then  $F_2(x)$  should decrease as  $(1-x)^p$  for  $x \rightarrow 1$ , where  $2n = p+1$ . In our case from (27)  $n = 3/2$ , hence  $p = 2$  and this agrees with (28), since  $\psi(\rho) \sim (1-\rho)$ , and  $q(\rho) \sim (1-\rho)^2$ .

## V. NUMERICAL SOLUTION

The equation (13) is the linear differential equation of the elliptic type. Boundary conditions are given in (14) and are compatible with the singularities of coefficients  $A_i$ . We have not succeeded in finding any analytic function, describing the main features of the solution, for example, one can demonstrate that simple ansatz  $\psi(\rho, t) = \phi(\rho) \cdot \xi(t)$  is not a solution of (13). Therefore we admitted two numerical procedures: a direct solution of (13) using discretization and a variational ansatz with the expansion of the solution into a complete set of functions of two variables. We have found that the former procedure turned out to be unstable and not accurate. We discuss below only the numerical results obtained in the framework of the second method.

The  $\Psi$  function in (13) depends on parameters  $m_1, m_2$  (bare quark masses),  $\sigma$  (string tension), 2 parameters  $y$  and  $\alpha$  defining the string parameter  $\tilde{y}$  (see (8)). The  $\Psi$  also depends on quantum numbers:  $L_z$ , total momentum  $L$  and radial quantum number  $N_r$ . The eigenvalue of (13) is the bound state mass squared  $M^2(L_z, L, N_r, y, \alpha)$ . We expand  $\Psi$ -function into the complete set of functions ( $\kappa = L_z, L, N_r$ ):

$$\Psi_\kappa(\rho, t) = \exp(iL_z \phi) \sum_{m=1}^\infty \sum_{n=0}^\infty C_{mnl}^\kappa \psi_{mnl} \quad (32)$$

where

$$\psi_{mnl}(\rho, t) = \sin(\pi m \rho) t^{\frac{1}{2}} L_n^l(\epsilon t) \exp(-\epsilon t/2). \quad (33)$$

Here  $\phi$  is the azimuthal angle of the corresponding angular motion in the  $xy$ -plane and  $L_n^l$  – Laguerre polynomials. The variational parameter  $\epsilon$  and the definition  $l \equiv L_z$  were also introduced. The basis functions are orthonormalized as:

$$\begin{aligned} \int_0^\infty \frac{dt}{2} \int_0^{2\pi} d\phi \int_0^1 d\rho \psi_{m'n'l'}^* (\rho, t) \psi_{mnl}(\rho, t) = \\ = \delta_{m'm} \delta_{n'n} \delta_{l'l} \frac{\pi}{2\epsilon^{l+1}} \frac{(n+l)!}{n!} \end{aligned} \quad (34)$$

and the total function is normalized as:

$$\int dV |\Psi|^2 = 1 \quad dV = \frac{1}{2} d\rho dt d\phi \quad (35)$$

Note, that each function  $\psi_{mnl}$  satisfies boundary conditions (14). We have used typically seven sine functions ( $m = 1, \dots, 7$ ) and seven Laguerre polynomials, which was compatible with the accessible computer time. The eigenvalue equation (13) was transformed into  $49 \times 49$  matrix equation and solved in a standard way. In some cases in order to check sensitivity of the procedure also other sets have been used, i.e.  $5 \times 9$  instead of  $7 \times 7$  and consistency of results was confirmed.

One important remark should be done here. The basis we have used is not large enough to analyze highly excited states with quantum numbers much more than unity because of loss of the accuracy. But in this region powerful quasiclassical methods may be applied in order to get the solution. Indeed, one of the main questions we are going to solve is to compare the spectra of light-cone Hamiltonian and center of mass one for the same dynamical problem: two massive spinless quarks connected by the straight-line string. In 1+1 case it is known for a long time [14], that light-cone and center of mass Hamiltonians for this problem are quasiclassically equivalent. It is reasonable to assume the quasiclassical equivalence in 3+1 case too. Therefore the main interest should be concentrated on the lowest states and the numerical procedure we have used is mostly adequate namely for the lowest states.

The resulting eigenvalues  $M^2(\kappa, y, \alpha)$  were ordered in their magnitude and for each state separately the minimizing value of  $y, \alpha$  was found. The orthogonality of the resulting wave functions for minimized parameters was then checked and appeared to be around few percents or better for all states except two. The latter belonged to almost degenerate states and the orthogonalization procedure for them is made easily.

The two-dimensional wave functions have been computed for minimized eigenvalues and formfactors and structure functions are computed according to the formulae of Section 4.

## VI. DISCUSSION OF RESULTS

We have chosen six sets of quark mass parameters, including 4 sets of equal masses and 2 sets of unequal masses as shown in Table I. (all masses are in units of GeV). The values of parameters  $y, \alpha, \epsilon$  are obtained by minimization procedure as explained in the previous section. The eigenstates obtained by our numerical procedure, explained in Section 6, are listed in Table II and shown as Fig. 1.

Let us first discuss the light-cone spectrum. The Hamiltonian (1) depends explicitly on  $L_z$ , whereas the Lorentz-invariance requires that masses do not depend on  $L_z$ , but depend on  $L$ . Consequently one expects that the lowest state for  $L_z = 0$  corresponds to  $L = 0$ , while the next state with  $L_z = 0$  corresponds to  $L = 1$  and must be degenerate in mass with the state  $L_z = 1, L = 1$ . This is clearly seen in Table II and Fig.1. The next triplet of states with  $L_z = 0, 1, 2$  should correspond to  $L = 2$ . Two of these states are found by us and minimized, while the third is not minimized since the procedure for this state was extremely time-consuming. As a result two states for  $L = 2$  listed in Table II and Fig. 1 are degenerated within 2% accuracy, while the third state is some 12% up (but should come down after minimization). The same feature is roughly present for  $L = 3, 4$  states where

we have only one minimized state for each  $L$ .

At this point one should take into account another degeneration – the dynamical one, and to this end discuss first center-of-mass spectrum, obtained from the c.m. Hamiltonian [8] or by numerical diagonalization of the string equation of motion [9]. We have computed the c.m. spectrum using the routine from [15]. The c.m. Hamiltonian for  $L = 0$  reduces to the so-called spinless Salpeter equation [16] which was actually solved by us. The approximate form of the spectrum which can be easily computed also by the WKB method [17] can be represented as:

$$\left(M^{(0)}(L, N_r)\right)^2 \cong 2\pi\sigma \left(2N_r + \frac{4}{\pi}L + \frac{3}{2}\right) \quad (36)$$

For  $L > 0$  one should take into account the string contribution, absent in spinless Salpeter equation but present in the Hamiltonian [6] and in [9]. This correction found in [9] is:

$$\Delta M = -\frac{16}{3}\sigma^2 \frac{L(L+1)}{(M^{(0)})^3} \quad (37)$$

The corrected masses,  $M(L, N_r) = M^{(0)} + \Delta M$  are shown in Table II and Fig.1. They are very close to the values computed in [9]. Now one can see that there is an approximate degeneration in mass  $M = M^{(0)} + \Delta M$  of states when one replaces one unit of  $N_r$  by two units of  $L$ . This is seen in Table II and even better in [18]. The same type of approximate mass degeneration is seen in the light-cone spectrum – compare e.g. the states with  $(N_r, L, L_z) = (1, 0, 0)$ ;  $M_{LC} = 2.25$  and  $(0, 2, 0)$ ;  $M_{LC} = 2.28$ .

In Fig.1 this degeneration is visualized as the fact that masses appear on the vertical lines. This degeneration is a dynamical one and is a characteristic feature of non-relativistic oscillator. In our relativistic case it reveals a new string – like symmetry, typical for the QCD string spectrum [18].

Let us now compare the light-cone and the center-of-mass spectrum. One could expect the coincidence up to an overall shift due to the different treatment of Z-graphs in two systems. In the c.m. Hamiltonian these Z-graphs are presented but supposed to be unimportant on the grounds, that the backtracking of a quark in time necessarily brings about a folding in the string world sheet which costs a large amount of action and is therefore suppressed. The situation is different in the light cone – it is general belief that Z-graphs are absent here. One also expects that the Z-graphs (and the overall shift) should decrease if quark masses are increasing.

The comparison of the spectra can be made from Table II and Fig.1. One can see indeed some overall shift down in the c.m. spectrum by some 0.1 GeV and otherwise the masses coincide within the accuracy of computation. This fact is highly nontrivial since two quantum Hamiltonians (the light-cone and center-of-mass ones)

are very different, they cannot be obtained from each other by a simple boost or other simple transformation. The light-cone Hamiltonian is rather complicated and it took the authors more than a year to get reasonable numerical results for it.

We have also checked the quark mass dependence of the overall shift of spectra and proved that it drops sharply with the quark mass increasing see Fig. 2, supporting the idea, that the shift is due to different treatment of Z graphs (or self energy graphs). This fact also confirms, that the shift is not a consequence of some systematic errors of our procedure. In that case one should expect the decreasing of relative mass difference, i.e.  $\delta M/M$  with the quark mass increasing and not the decreasing of absolute difference  $\delta M$ , which has been actually observed.

We now turn to eigenfunctions. One expects in this case two types of excitation: the radial one leading to new nodes on  $\rho$  coordinate and similar to the 1+1 excited states and the  $r_\perp$ -excitation which causes nodes in the  $t$ -coordinate and associated with the orbital excitation. This is clearly seen in Fig. 3, where (a) refers to the ground state, (b) – to the orbital and (c) – to the radial excitation. A more complicated example, combining both types of excitation is given in Fig. 3 (d).

As the next illustration we show in Fig. 4 the case of two heavy quarks, demonstrating two types of excitation and also a new feature – the actual region of parameters is squeezed to a small region near  $\rho = 1/2$ . In Fig. 5 we demonstrate four states for the case of unequal masses – the "physical region" is shifted to one of the ends of the  $[0,1]$  interval.

At this point it is important to find connection of our light-cone wave function to the nonrelativistic one, usually defined in the c.m.. In [8] it was demonstrated that this connection can be established only when both quarks are heavy,  $m_1, m_2 \gg \sqrt{\sigma}$ . In this case  $\tilde{y} \ll 1$  (as can be found by direct minimization of the Hamiltonian (1)) – the string transforms into the potential and loses its material and momentum contents. One can introduce as in [8] the relative momentum  $p_z$  and relative coordinate  $r_z$ :

$$p_z = (m_1 + m_2) \left( x - \frac{m_1}{m_1 + m_2} \right) \quad (38)$$

$$r_z = \frac{P_+ r_-}{m_1 + m_2} \quad (39)$$

and the  $M$  operator can be written as:

$$M \approx m_1 + m_2 + \frac{1}{2\tilde{m}}(\vec{p}_\perp^2 + \vec{p}_z^2) + \sigma \sqrt{r_\perp^2 + r_z^2} \quad (40)$$

Hence one can write the momentum-space nonrelativistic wave function  $\Psi(\vec{p}^2)$  directly through the light-cone variables:

$$\Psi(\vec{p}^2) = \Psi \left[ p_\perp^2 + (m_1 + m_2)^2 \left( x - \frac{m_1}{m_1 + m_2} \right)^2 \right] \quad (41)$$

This representation is valid in the large mass limit  $m_i \gg \sqrt{\sigma}$  stated above and in addition near the center of the  $x$ -distribution, i.e. when  $|x - m_1/(m_1 + m_2)| \ll 1$ . The width of the peak in  $x$  variable is proportional to  $(m_1 + m_2)^{-2}$  and is very narrow for heavy quarks. The form (38) is not correct for  $x$  at the ends of the interval, i.e.  $x = 0, 1$  (remember that for large  $m_i$  the extremum value of  $\tilde{y}$  tends to zero and  $x = \rho$  changes in the interval  $[0,1]$ ). Indeed the exact wave function as discussed in Section 4 vanishes linearly at  $x = 0, 1$ , while the r.h.s of (41) stays nonzero. Moreover, the Jacobean  $\mathcal{J}$  of the phase space  $d^3p = \mathcal{J} dx d^2p_\perp$  is constant  $\mathcal{J} = m_1 + m_2$  and does not change this conclusion.

The correspondence of the c.m. and light-cone wave functions is lost if quark masses  $m_i$  are of the order of  $\sqrt{\sigma}$  or less. The physical reason is that the role of dynamics is now 100% important and the dynamics is different in different frames: the light-cone Hamiltonian and wave functions are connected with those of the center-of-mass by a dynamical transformation, which includes nonkinematical Poisson operators. Hence one cannot hope to obtain one wave function from another using only transformation including the kinematical (free) part of the operator  $M^2$ . Moreover, a glance at the operator  $M^2$  in (1) helps to realize that the separation of  $M^2$  into the purely kinetic part (containing only momentum and masses) and purely potential one (containing only relative coordinates) is impossible at all: e.g. the string enters through the term  $(P_+ r_-)^2$  and mixed terms like  $p_\perp r_\perp$  are present everywhere. This circumstance limits the use of simple recipes known in literature [7], which connect the c.m. and light-cone wave functions. In particular, the ansatz for  $p_z$  suggested in [7] and used for equal quark masses

$$p_z = \sqrt{\frac{m^2 + k_\perp^2}{x(1-x)}} \left( x - \frac{1}{2} \right) \quad (42)$$

coincides with our form (39) rigorously derived in [6] only for large  $m$ ,  $m \gg \sqrt{\sigma}$  and  $x$  in the narrow region around  $x = 1/2$  but differs at the tails of the wave function. For light quark masses,  $m \leq \sigma$  and small  $p_\perp$  the relation (42) yields incorrect results which can be seen in the almost constant behaviour in the interval  $[0,1]$  of the light-cone wave function, produced by the insertion of (42) into the c.m. wave function, typically

$$\psi(\vec{p}^2) \sim \exp(-a^2 \vec{p}^2) \rightarrow \exp(-a^2 [p_\perp^2 + \frac{m^2 + p_\perp^2}{x(1-x)} (x - \frac{1}{2})^2])$$

is insensitive to  $x$  for  $m, p_\perp \rightarrow 0$ , whereas the exact light-cone wave function is decreasing as  $x(1-x)$ , see Fig. 6.

At the same time for heavy quark masses,  $m \gg \sqrt{\sigma}$  the two functions, one transformed by (42) from the c.m. and another is a genuine light-cone wave-function solution of (13), are very close to each other. This can be seen in Fig. 7 for  $m = 1.4$  GeV.

We now turn to the formfactor of computed states 1-4, see Table I, presented in Fig. 6. The main feature of the Fig. 6 is a very slow decrease of  $F(q^2)$  with  $q^2$  which signals in particular a small radius of states. Indeed the values of  $\sqrt{\langle r^2 \rangle}$  are too low ( $\sim 0.338 \text{ fm}$  for massless quarks). This fact is in agreement with the earlier c.m. calculations of [19].

Note that color Coulomb and spin interaction can only decrease radius. In the same Fig. 8 are also shown formfactor calculated in the c.m. system for the equal mass values listed in Table I (cases 1-4). These formfactors can be calculated either in terms of light-cone variables as in [7] and [11], or simply using the nonrelativistic expression

$$F(q^2) = \int |\psi_{cm}(r)|^2 \frac{\sin(qr/2)}{qr/2} d^3r \quad (43)$$

since both integrals can be transformed one into another by a change of variables. One can see in Fig. 8, that the c.m. formfactor is systematically below that of the light-cone.

Finally we turn to the quark-distribution function  $q(\rho)$ . It is computed through the light-cone wavefunction  $\psi(\rho, t)$  using (28) and shown in Fig. 9. One can see the symmetric behaviour of  $q(\rho)$  with respect to reflection  $\rho \rightarrow 1 - \rho$ . At the ends of the interval  $q(\rho)$  vanishes like  $\rho^2$  and  $(1 - \rho)^2$ , in the agreement with the  $1/q^3$  behaviour of the formfactor at large  $q$  due to the Drell-Yan-West relations [13].

Note the narrowing of the peak in  $q(\rho)$  in Fig. 9 for increasing quark masses.

## VII. CONCLUSION

The present paper is the first in the planned series of papers devoted to the systematic study of nonperturbative contribution to formfactors, quark distributions and high-energy scattering amplitudes.

The main physical idea of our approach is that the most part of nonperturbative dynamics in QCD is due to the QCD string, and the latter is described by the Nambu-Goto part of the Hamiltonian, which was written before in the c.m. [8] as well as in the light-cone coordinates [6].

Only valence part of the Fock's column was considered above in the paper, also for simplicity spins and perturbative gluon exchanges are neglected. To do the systematic comparison with experiment all these three simplifications should be eliminated. Let us discuss their effect point by point. The higher Fock states are necessary to reproduce the Regge behaviour of  $q(x) \sim x^{-\alpha_\rho(0)}$  at small  $x$  (and at  $x \rightarrow 1$  for quark distributions of hadrons in high-energy scattering). Here comes the first crucial point; to be answered in the second paper of this series, what is the QCD reggeon?

In our method the higher Fock states, constituting the QCD reggeon, correspond to several gluons propagating in the nonperturbative background and therefore confined to the excited Nambu-Goto surface [20]. These states are in one-to-one correspondence with the excited Nambu-Goto string states. This is the picture at large distances; at small distances smaller than the vacuum correlation length (width of the Nambu-Goto string)  $T_g \sim 0.2 \text{ fm}$  [21], the string disappears and the usual perturbative gluon exchanges reappear.

The effect of spin of light quarks is highly nontrivial [5]. It leads to the creation of the new vertex, which yields the constituent quark structure. Physically one may imagine this structure as being due to the light-quark walks around the end of the string.

Having said all this, what is the lesson of the present work and of its possible development?

The first lesson is that valence quark component can be successfully dynamically computed on the light cone; the string on the light cone is physically and mathematically well defined. The spectrum obtained on the light cone for the first time reasonably coincides with that of the c.m. Hamiltonian for the string with quarks. Moreover, the nonperturbative wave function obtained directly on the light cone allows to calculate nonperturbative contributions to the formfactor and structure function.

The second lesson is that the formfactor computed directly on the light cone is close to of c.m. for small  $q$  (see Fig. 7), but is systematically above the c.m. formfactor for larger  $q$ . This is not surprising, since in the light-cone formfactor there is a mechanism of the "redistribution" of the momentum  $q$  between the quarks, since  $q$  enters the light-cone formfactor (25) multiplied with  $(1 - x)$ , so that the larger  $q$ , the smaller is  $(1 - x)$  and the wave function does not decrease too fast. Physically it means that at large  $q$  the configuration survives where the spectator quark gets as little momentum as possible so that it can be easily turned together with the active quark. This is exactly what is called the Feynman mechanism [1].

The third lesson is that the minimal string plays only a passive role on the light cone, namely it participates in sharing of the total momentum and carries the part equal to  $\langle \tilde{y} \rangle$ , but it does not produce the  $x$ -distribution in structure function, which could simulate the gluonic structure function. The reason is that the string variable - the einbein field  $\nu$  - is quasiclassical and has no dispersion.

The value of  $\langle \tilde{y} \rangle$  computed according to (31) depends on quark masses and is listed in Table. I. It is reasonable that  $\langle \tilde{y} \rangle = 0.22$  is smaller than the experimental value of overall gluon momentum, 0.55, since in our picture the difference should be filled in by higher Fock components.

The fourth lesson comes from the comparison of the computed quark distribution, Fig. 9, with the experimental data for the pionic structure function [22]. Behaviour of  $q(\rho)$  at small  $\rho$  and small  $(1 - \rho)$  is symmetric in Fig. 9, while in reality  $q(x)$  should rise at small  $x$  like



$x^{-\alpha\rho(0)} \sim x^{-0.5}$  (we neglect at this point the difference between  $x$  and  $\rho$ , which is due to  $\langle \tilde{y} \rangle$ ). This peak at the small  $x$  should be filled in by the contribution of higher Fock components, containing additional gluons on the string, as was discussed above. The behaviour of  $q(\rho)$  at  $\rho = 1$ , which is calculated to be  $(1 - \rho)^2$  will be also changed into  $(1 - \rho)$  due to gluon exchanges, which account for the formfactor asymptotic  $1/q^2$  at large  $q$ , and the Drell-Yan-West duality ensure the  $(1 - \rho)$  behaviour around  $\rho = 1$ .

Finally, the formfactor calculated above in the paper, Fig. 8 shows too little radius of the "pion"  $\langle r^2 \rangle \approx (0.34 \text{ fm})^2$  as compared with the experimental one  $\langle r^2 \rangle \approx (0.67 \text{ fm})^2$ . This fact is in qualitative agreement with other calculations, where the c.m. wave-function was used [19], and some authors assumed as in [4] that quarks have "internal" structure and their own radius which should be added to the "body radius" to reproduce the experimental value. This fact of small body radius seems to be a necessary consequence of the simple string + point-like quarks picture, and probably cannot be cured by the higher Fock components.

The calculation of the quark structure as produced by the spin and chiral effects is thus an interesting and fundamental problem which will be discussed in another paper of this series.

#### ACKNOWLEDGMENTS

The calculations of the c.m. wave-function have been done using the codes by B.L.G. Bakker, the Free University of Amsterdam. The authors are very grateful to him for the submitting of his codes and valuable explanations.

The authors are grateful to A.B. Kaidalov for numerous discussion of QCD reggeon picture, and to Yu.S. Kalashnikova and A. Nefediev for discussions concerning different questions of hamiltonian dynamics and to V.A. Novikov for useful comments.

This work was supported in part by the RFFI grant N 96-02-19184a and 95-048-08. Yu.S. was supported in part by the INTAS grant 93-79.

#### APPENDIX A:

This appendix is based on the material of Ref. [6]

Given a  $q\bar{q}$  Green's function in the coordinate space  $G(x\bar{x}; y\bar{y})$ , where  $x\bar{x}(y\bar{y})$  are final (initial) 4-coordinates of quark and antiquark, one can define the Hamiltonian  $H$  through the equation (in the euclidean space-time)

$$\frac{\partial G}{\partial T} = -HG \quad (\text{A.1})$$

where  $T$  is an evolution parameter corresponding to some choice of a hypersurface  $\Sigma$ . In a particular case of the

c.m. Hamiltonian the role of  $T$  is played by the center-of-mass euclidean time coordinate  $T = (x_4 + \bar{x}_4)/2$  and the hypersurface  $\Sigma$  is a hyperplane  $x_4 = \bar{x}_4 = \text{const}$ .

With the notations for the vectors  $a_\mu, b_\mu$

$$ab = a_\mu b_\mu = a_i b_i - a_0 b_0 = a_\perp b_\perp + a_+ b_- + a_- b_+,$$

$$a_\pm = \frac{a_3 \pm a_0}{\sqrt{2}},$$

one can define the hypersurface  $\Sigma$  through the  $q\bar{q}$  coordinates  $z_\mu, \bar{z}_\mu$  as

$$z_+(\tau) = \bar{z}_+(\bar{\tau})$$

and the kinetic part of the action  $A$

$$A = K + \bar{K} + \sigma S_{min},$$

has the form

$$\begin{aligned} K + \bar{K} &= \frac{1}{4} \int_0^s \dot{z}_\mu^2(\tau) d\tau + \\ &+ \frac{1}{4} \int_0^{\bar{s}} \dot{\bar{z}}_\mu^2(\bar{\tau}) d\bar{\tau} + \int_0^s m_1^2 d\tau + \int_0^{\bar{s}} m_2^2 d\tau = \\ &= \int_0^T dz_+ \left[ \frac{\mu_1}{2} (\dot{z}_\perp^2 + 2\dot{z}_-) + \right. \\ &\left. + \frac{\mu_2}{2} (\dot{\bar{z}}_\perp^2 + 2\dot{\bar{z}}_-) + \frac{m_1^2}{2\mu_1} + \frac{m_2^2}{2\mu_2} \right] \end{aligned}$$

where we have defined

$$2\mu_1(z_+) = \frac{\partial z_+}{\partial \tau}; \quad 2\mu_2(z_+) = \frac{\partial \bar{z}_+}{\partial \tau}$$

The minimal surface  $S_{min}$  is formed by connecting  $z_\mu(z_+)$  and  $\bar{z}_\mu(z_+)$  with the same value of the evolution parameter  $z_+$ , i.e.

$$S_{min} = \sigma \int_0^T dz_+ \int_0^1 d\beta [\dot{w}^2 w'^2 - (\dot{w} w')^2]^{1/2}$$

where

$$w_\mu(z_+; \beta) = z_\mu(z_+) \beta + \bar{z}_\mu(z_+) (1 - \beta)$$

and dot and prime denote derivatives in  $z_+$  and  $\beta$  respectively throughout this Appendix.

We now introduce "center-of-mass" and relative coordinates,

$$\dot{R}_\mu = x \dot{z}_\mu + (1 - x) \dot{\bar{z}}_\mu, \quad \dot{r}_\mu = \dot{z}_\mu - \dot{\bar{z}}_\mu$$

where the variable  $x$  is defined from the requirement that the term  $\dot{r}_\perp \dot{R}_\perp$  should be absent in the action. This yields:

$$x = \frac{\mu_1 + \int \nu \beta d\beta}{\mu_1 + \mu_2 + \int \nu d\beta}$$

Then for the Green function one obtains:

$$G(x\bar{x}; y\bar{y}) = \int D\mu_1(z_+) D\mu_2(z_+) D\nu DR_\mu Dr_\mu e^{-A}$$

where the action  $A$

$$A = \frac{1}{2} \int dz_+ \left\{ \frac{m_1^2}{\mu_1} + \frac{m_2^2}{\mu_2} + a_1(\dot{R}_\perp^2 + 2\dot{R}_-) + a_3\dot{r}_\perp^2 + \int \frac{\sigma^2}{\nu} d\beta r_\perp^2 - \frac{(r_- + \dot{R}_\perp r_\perp + (\langle \beta \rangle - x)\dot{r}_\perp r_\perp)^2}{r_\perp^2 (\int \nu d\beta)^{-1}} - \frac{(\dot{r}_\perp r_\perp)^2 \int \nu(\beta - \langle \beta \rangle)^2 d\beta}{r_\perp^2} \right\}, \quad (\text{A.})$$

The following notation was used:

$$a_1 = \mu_1 + \mu_2 + \int_0^1 \nu(\beta) d\beta$$

$$a_3 = \mu_1(1-x)^2 + \mu_2 x^2 + \int_0^1 \nu(\beta)(\beta-x)^2 d\beta$$

Integration over  $DR_\mu$  leads to an important constraint:

$$a_1 = P_+$$

Furthermore we go over into the minkowskian space, which means that

$$\mu_i \rightarrow -i\mu_i^M, \quad \nu \rightarrow -i\nu^M$$

$$a_i \rightarrow -ia_i^M, \quad A \rightarrow -iA^M$$

For the minkowskian action we obtain (omitting from now on the superscript  $M$  everywhere)

$$A^M = \frac{1}{2} \int dz_+ \left\{ -\frac{m_1^2}{\mu_1} - \frac{m_2^2}{\mu_2} + a_3\dot{r}_\perp^2 - \int \frac{\sigma^2 d\beta}{\nu} r_\perp^2 - \nu_2 \frac{(\dot{r}_\perp r_\perp)^2}{r_\perp^2} - \frac{\nu_0 a_1}{(\mu_1 + \mu_2)r_\perp^2} [r_- + (\langle \beta \rangle - x)\dot{r}_\perp r_\perp]^2 \right\}$$

and using (4) one easy obtains the Hamiltonian (1) which opened the main text.

To complete the Hamiltonian formulation of our problem we define canonical momenta for the coordinates  $\dot{R}_-$

and  $\dot{r}_-$ . As it was shown, canonically conjugated momentum to the  $\dot{R}_-$  is  $P_+ = a_1$ . Situation with  $\dot{r}_-$  is more subtle. In order to clarify the situation let us start with the general form of the  $q\bar{q}$  Green's function in the Feynman-Schwinger formalism

$$G(x, y) = \int ds d\bar{s} Dz D\bar{z} e^{-K - \bar{K}} \langle W(C) \rangle$$

to impose boundary conditions, one can rewrite  $Dz D\bar{z}$  using discretization

$$\xi_n \equiv z(n) - z(n-1), \quad \bar{\xi}_n \equiv \bar{z}(n) - \bar{z}(n-1)$$

$$Dz D\bar{z} = \prod_{n, n'} d\xi_n d\bar{\xi}_{n'} dp dp' \times$$

$$\times \exp \left\{ ip \left( \sum \xi_n + X - Y \right) + ip' \left( \sum \bar{\xi}_{n'} + X - Y \right) \right\}$$

One can introduce the total and relative momenta

$$P = p + p', \quad q = \frac{p - p'}{2};$$

and  $\dot{R} = \Delta R_n / \varepsilon$ ;  $N\varepsilon = T$ , one has

$$\xi_n x_n + \bar{\xi}_n (1 - x_n) = \Delta R_n$$

$$\xi_n - \bar{\xi}_n = \Delta r_n$$

Expressing  $\xi_n, \bar{\xi}_n$  through  $\Delta R_n, \Delta r_n$  and going over to the momentum representation of  $G$  one obtains

$$G(P) = \int dq \prod_{n, n'} d\Delta R_n d\Delta r_{n'} \times$$

$$\times \exp \left\{ iA + iP \sum_n \Delta R_n + i \sum_n \left( \frac{1}{2} P(1 - 2x) + q \right) \Delta r_n \right\}$$

where  $A = \int_0^T d\tau \mathcal{L} = \int_0^T d\tau (K + \bar{K} - \sigma S_{min})$  One can now introduce the Hamiltonian form of the path integral via

$$\int Dx e^{i \int \mathcal{L} d\tau} = \int Dx Dp e^{ip_k \dot{x}_k - i \int \mathcal{H} d\tau}$$

and rewrite the first two exponents as

$$\exp \left\{ i \int P_i \dot{R}_i d\tau + i \int \left[ \frac{1}{2} P_i (1 - 2x(\tau)) + q_i \right] \dot{r}_i d\tau \right\}$$

The term proportional  $q_i$  disappears because of boundary conditions  $r_\mu(0) = r_\mu(T) = 0$ , and one obtains

$$p_+ = \frac{1}{2} P_+ (1 - 2x), \quad [p_+, r_-] = -i$$

One can rewrite this in the form

$$P_+ r_- = i \frac{\partial}{\partial x}, \quad [P_+ r_-, x] = i$$

## APPENDIX B:

The aim of this appendix is to derive the Eq.(13) from Eq.(1). The first thing to do is to express the Hamiltonian (1) as :

$$H = \frac{M^2}{2P_+} \quad (\text{B.1})$$

Then using definition (3) we obtain the following form for  $M^2$ :

$$M^2 = \left\{ \frac{m_1^2}{x - \tilde{y}_0 \langle \beta \rangle} + \frac{m_2^2}{1 - x - \tilde{y}_0(1 - \langle \beta \rangle)} + \frac{L_z^2}{\tilde{c} r_\perp^2} + \left[ \frac{1}{x - \tilde{y}_0 \langle \beta \rangle} + \frac{1}{1 - x - \tilde{y}_0(1 - \langle \beta \rangle)} \right] \times \frac{[p_\perp r_\perp + \tilde{\gamma}(P_+ r_-)]^2}{r_\perp^2} + \int \frac{\sigma^2}{\tilde{y}} r_\perp^2 d\beta + \frac{\tilde{y}_0}{1 - \tilde{y}_0} \frac{(P_+ r_-)^2}{r_\perp^2} \right\} \quad (\text{B.2})$$

here

$$\tilde{c} = (x - \tilde{y}_0 \langle \beta \rangle)(1 - x)^2 +$$

$$[1 - x - \tilde{y}_0(1 - \langle \beta \rangle)]x^2 + \int_0^1 \tilde{y}(\beta - x)^2 d\beta$$

and

$$\tilde{\gamma} = \frac{\tilde{y}_0}{1 - \tilde{y}_0} (\langle \beta \rangle - x)$$

As it was mentioned above, it is more convenient to express  $M^2$  through a new variable  $\rho$ :

$$\rho = \frac{1}{1 - \tilde{y}_0} (x - \tilde{y}_0 \langle \beta \rangle)$$

Substituting this variable into (B.2) one obtains:

$$M^2 = \frac{1}{1 - \tilde{y}_0} \left\{ \frac{m_1^2}{\rho} + \frac{m_2^2}{1 - \rho} + \frac{L_z^2}{\tilde{c} t} + \left( \frac{1}{\rho} + \frac{1}{1 - \rho} \right) \times \frac{[p_\perp r_\perp + \tilde{\gamma}(P_+ r_-)]^2}{t} + (1 - \tilde{y}_0) \int \frac{\sigma^2}{\tilde{y}} t d\beta + \frac{\tilde{y}_0 (P_+ r_-)^2}{t} \right\} \quad (\text{B.3})$$

where the notation  $t = r_\perp^2$  was used.

Quantization of the above expression is done according to the canonical commutation relations:

$$\{p_\perp^k, r_\perp^j\} = -i\delta^{kj}$$

$$\{x, (P_+ r_-)\} = -i$$

We are looking for the wave function of the problem given in the mixed coordinate - momentum representation  $\psi = \psi(\rho, t)$ , so one has to substitute into (B.3) the operators:

$$(P_+ r_-) = i \left( \frac{1}{1 - \tilde{y}_0} \right) \frac{\partial}{\partial \rho} ; p_\perp^k = -i \frac{\partial}{\partial r_\perp^k}$$

The important point is the operators ordering. We use the Weil ordering rule, i.e.

$$AB \rightarrow \frac{1}{2}(\hat{A}\hat{B} + \hat{B}\hat{A})$$

for any noncommuting operators  $A$  and  $B$ . Let us notice that  $\tilde{y}$  explicitly depends on  $t$  according to (8) and hence should also be differentiated during the ordering procedure. The final result for the operator  $\hat{M}^2$  may be found by the straightforward calculations, it is

$$\hat{M}^2 = A_1 \frac{\partial^2}{\partial t^2} + A_2 \frac{\partial^2}{\partial \rho^2} + A_3 \frac{\partial^2}{\partial t \partial \rho} + A_4 \frac{\partial}{\partial t} + A_5 \frac{\partial}{\partial \rho} + A_6 \quad (\text{B.4})$$

where the coefficients  $A_i$  :

$$A_1(\rho, t) = -\frac{4t}{\rho(1 - \rho)} \frac{1 + \alpha t}{[1 + (\alpha - y)t]}$$

$$A_2(\rho, t) = -\frac{y(1 + \alpha t)}{[1 + (\alpha - y)t]^3} \left[ yt \frac{(\rho - \langle \beta \rangle)^2}{\rho(1 - \rho)} + 1 + \alpha t \right]$$

$$A_3(\rho, t) = -4yt \frac{(1 + \alpha t)}{[1 + (\alpha - y)t]^2} \frac{(\rho - \langle \beta \rangle)}{\rho(1 - \rho)}$$

$$A_4(\rho, t) = -\frac{1}{\rho(1 - \rho)} \times$$

$$\times \left\{ 4 \frac{yt}{[1 + (\alpha - y)t]^2} + 4 \frac{1 + \alpha t}{1 + (\alpha - y)t} + 2yt \frac{(1 + \alpha t)}{[1 + (\alpha - y)t]^2} \frac{(\rho^2 - 2\rho \langle \beta \rangle + \langle \beta \rangle)}{\rho(1 - \rho)} \right\}$$

$$A_5(\rho, t) = -2y \frac{[1 + (\alpha + y)t]}{[1 + (\alpha - y)t]^3} \frac{(\rho - \langle \beta \rangle)}{\rho(1 - \rho)}$$

$$\begin{aligned}
& -y^2 t \frac{(1+\alpha t)}{[1+(\alpha-y)t]^3} \times \\
& \times \frac{(\rho - \langle \beta \rangle)[(\rho(1-2\langle \beta \rangle) + \langle \beta \rangle)]}{[\rho(1-\rho)]^2} \\
A_6(\rho, t) = & \frac{1+\alpha t}{1+(\alpha-y)t} \left( \frac{m_1^2}{\rho} + \frac{m_2^2}{1-\rho} \right) + \frac{1+\alpha t}{y} + \\
& + \frac{L_z^2 (1+\alpha t)^2}{t a_6} - \frac{y^2 t (1+\alpha t)}{[1+(\alpha-y)t]^3} \times \\
& \times \frac{[\rho^3(1-2\langle \beta \rangle) - 3\langle \beta \rangle^2 \rho(1-\rho) + \langle \beta \rangle^2]}{[\rho(1-\rho)]^3} - \\
& - \frac{y}{\rho(1-\rho)} \frac{[3 - (\alpha-y)t]}{[1+(\alpha-y)t]^3} - \\
& - y \frac{(\rho^2 - 2\langle \beta \rangle \rho + \langle \beta \rangle)}{[\rho(1-\rho)]^2} \frac{[1+(\alpha+y)t]}{[1+(\alpha-y)t]^3}
\end{aligned}$$

where:

$$\begin{aligned}
a_6 = & yt[1+(\alpha-y)t](\rho - \langle \beta \rangle)^2 + \\
& + [1+(\alpha-y)t](1+\alpha t)\rho(1-\rho) + yt(1+\alpha t)\gamma
\end{aligned}$$

- 
- [1] R.P. Feynman, in *Photon-Hadron interaction*, (Benjamin, New York, 1972); F.J. Ynduráin, in *The theory of Quark and Gluon Interactions*, (2nd edition, Springer, 1992); B.L. Iofe, V.A. Khoze, L.N. Lipatov, in *Hard Processes*, Vol. 1, (North Holland, 1984).
- [2] J. Kuti and V.F. Weisskopf, Phys. Rev. **D 4**, 3418 (1971).
- [3] G. Altarelli, N. Cabibo, L. Maiani and R. Petronzio, Nucl. Phys. **B 69**, 531 (1974).
- [4] G. Altarelli, S. Petrarca, F. Rapuano, Phys. Lett. **B 373**, 200 (1996).
- [5] Yu.A. Simonov, The Theory of Light Quarks in the Confining Vacuum, (in preparation).
- [6] A.Yu. Dubin, A.B. Kaydalov and Yu.A. Simonov, Phys. Lett. **B 343**, 310 (1995); [ Sov. J. Nucl. Phys. **58**, 348 (1995) ].
- [7] M.V. Terentiev, Sov. J. Nucl. Phys., **24**, 106 (1976); P.L. Chung, F. Coester and W.N. Polyzou, Phys. Lett. **B 205**, 545 (1988).
- [8] A.Yu. Dubin, A.B. Kaydalov and Yu.A. Simonov, Phys. Lett. **B 323**, 41 (1994);

- [9] D.La. Course and M.G. Olsson, Phys. Rev. **D 39**, 2751 (1989);  
M.G. Olsson and K. Williams, Phys. Rev. **D 48**, 417 (1993).
- [10] G.'t Hooft, Nucl. Phys. **B 75**, 461 (1974).
- [11] S.D. Drell and T.M. Yan, Phys. Rev. Lett. **24**, 181 (1970).
- [12] A.V. Radyushkin, Preprint CEBAF-TH-92-18, (1992); A.V. Radyushkin, Preprint CEBAF-TH-93-12, (1993); V. Braun, I. Halperin, MPI-PhT/94-08, (1994).
- [13] G.B. West, Phys. Rev. Lett. **24**, 1206 (1970).
- [14] I. Bars, A.J. Hanson, Phys. Rev. **D 13**, 1744 (1976); W.A. Bardeen, I. Bars, A.J. Hanson, R.D. Peccei, Phys. Rev. **D 13**, 2364 (1976); Phys. Rev. **D 14**, 2193 (1976); Yu.S. Kalashnikova and A. Nefediev, hep-th/9701193, Phys. Lett. **B**, in press.
- [15] B.L.G. Bakker, private communication.
- [16] W. Lucha and F.F. Schoeber, in *Quark Confinement and the Hadron Spectrum*, eds, N. Brambilla and G.M. Prosperi, (World Scientific, Singapore, 1994).
- [17] P. Cea, G. Nardulli and G. Preparata, Z. Phys. **C 16**, 135 (1982); P. Cea, G. Nardulli and G. Preparata, Phys. Lett. **B 115**, 310 (1982); J.L. Basdevant and S. Boukraa, Z. Phys. **C 28**, 413 (1985).
- [18] Yu.A. Simonov, in *Hadron '93*, eds. T. Bressani, A. Felicielli, G. Preparata and P.G. Ratcliffe, (Centro A. Volta, Como, 1993).
- [19] J. Carlson, J. Kogut and V.R. Pandharipande, Phys. Rev., **D 27**, 233 (1983).
- [20] Yu.A. Simonov, Yad. Fiz., **58**, 113 (1995); Yu.A. Simonov, in *Lecture Note in Physics*, vol 479, (Springer, 1997).
- [21] L.Del Debbio, A.Di Giacomo, Yu.A. Simonov, Phys. Lett, **B 332**, 11 (1994).
- [22] P.J. Sutton, A.D. Martin, W.J. Stirling and R.G. Roberts, Phys. Rev. **D 45**, 2349 (1992).

FIG. 1. The Chew-Frautschi plot with masses computed via the light-cone (circles, squares and triangle for  $L_z = 0, 1, 2$  respectively) and the c.m. Hamiltonian (stars). The systematic overall mass shift is seen as a divergence of straight lines passing through circles and stars. The states with high  $L$  or high  $N_r$  (daughter trajectories) are numerically less reliable and not shown.

FIG. 2. The systematic mass shift between mass eigenvalues of the light-cone and c.m. Hamiltonians versus quark mass.

FIG. 3. The 3d plots of wave functions of the four lowest states of light-cone Hamiltonian for zero quark masses. Coordinates on horizontal plane are  $0 \leq \rho \leq 1$ ,  $0 \leq t \leq 15$  (in units of  $\sigma^{-1}$ ).

FIG. 4. The same as in Fig. 3 but for heavy quark masses,  $m_1 = m_2 = 5$  GeV.

FIG. 5. The same as in Fig. 3 but for unequal quark masses,  $m_1 = 5$ ,  $m_2 = 0$  GeV.

FIG. 6. The 3d plots of the ground-state wave functions  $\Psi(\rho, t)$ , computed via the light-cone Hamiltonian (upper part) and via the c.m. Hamiltonian, with the standard substitution (42) (lower part) for zero quark masses.

FIG. 7. The same as in Fig.6 but for heavy quark masses,  $m_1 = m_2 = 1.4$  GeV.

FIG. 8. Formfactors calculated with light-cone wave-functions for the cases 1-4 of Table I (solid lines) and with the c.m. wave-functions (lines with stars).

FIG. 9. The quark-distribution function  $q(\rho)$  computed with light-cone wave-functions for the cases 1-4 of Table I.

TABLE I. Quark masses and minimizing values of variational parameters for six cases, computed in the paper together with  $\langle r^2 \rangle$  and  $\langle \tilde{y} \rangle$  for each case.

	$m_{q_1}$	$m_{q_2}$	$y$	$\alpha$	$\epsilon$	$\langle \beta \rangle$	$\langle \tilde{y} \rangle$	$\sqrt{\langle r^2 \rangle} fm$
Case 1	0.00	0.00	0.40	0.75	1.0	0.50	0.223	0.338
Case 2	0.25	0.25	0.35	0.75	1.0	0.50	0.190	0.329
Case 3	1.40	1.40	0.20	0.75	1.7	0.50	0.081	0.249
Case 4	5.00	5.00	0.10	1.50	3.5	0.50	0.017	0.1675
Case 5	1.40	0.00	0.20	0.50	1.1	0.10	—	—
Case 6	5.00	0.00	0.07	0.25	1.5	0.13	—	—

TABLE II. The light-cone mass eigenvalues (mass in L-C – the fourth column), and the c.m. mass eigenvalues without (mass in C-M – the fifth column) and with string correction ( $M^{(0)} - \Delta M$  in CM – the sixth column) The first 3 columns contain the quantum numbers assignment for the given state, and the last two columns – the minimizing values of variational parameters  $y$  and  $\alpha$ . All eigenvalues are computed for quark masses equal to 0.12 GeV. The masses marked by asterix are minimized with parametres  $y, \alpha$  listed in the last two columns.

$N_r$	$L$	$L_z$	Mass in L-C	$M^{(0)}$ in C-M	$M^{(0)} - \Delta M$ in C-M	$y$	$\alpha$
0	0	0	1.5704 *	1.4604	1.4604	0.40	0.80
0	1	0	2.0063 *	1.9236	1.8637	0.15	0.20
0	1	1	1.9926 *	—	—	0.40	0.80
0	2	0	2.2835 *	2.2990	2.1937	0.20	0.30
0	2	1	2.6138	—	—	0.40	0.80
0	2	2	2.3222 *	—	—	0.40	0.80
0	3	0	2.6574 *	—	—	0.10	0.30
0	3	1	3.1665	—	—	0.40	0.80
0	3	2	2.8157	—	—	0.40	0.80
0	4	0	3.0675 *	—	—	0.15	0.20
0	4	1	3.3175	—	—	0.40	0.80
0	4	2	3.3127	—	—	0.40	0.80
1	0	0	2.2567 *	2.1483	2.1483	0.20	0.40
1	1	0	2.6477 *	2.4728	2.4446	0.10	0.15
1	1	1	2.5909	—	—	0.40	0.80
1	2	1	3.0787	—	—	0.40	0.80
1	2	2	2.8879	—	—	0.40	0.80
2	0	0	2.9298 *	2.6707	2.6707	0.10	0.20

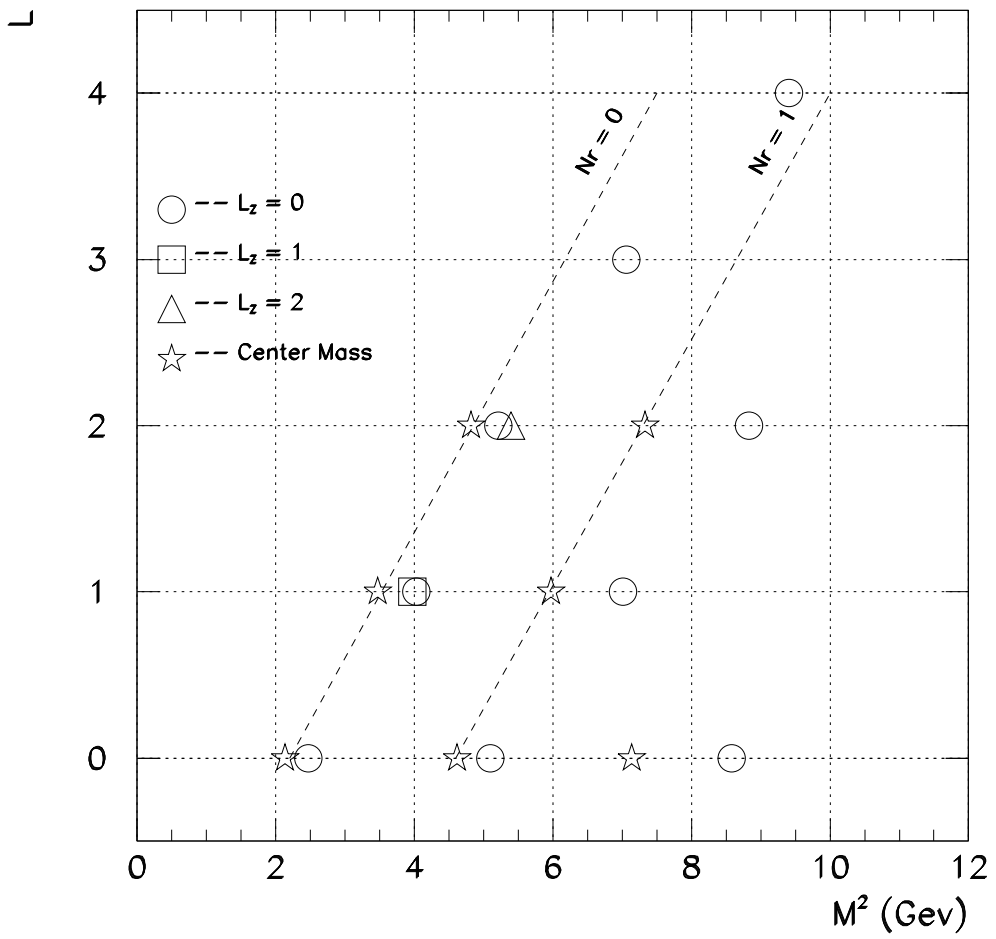


Fig. 1

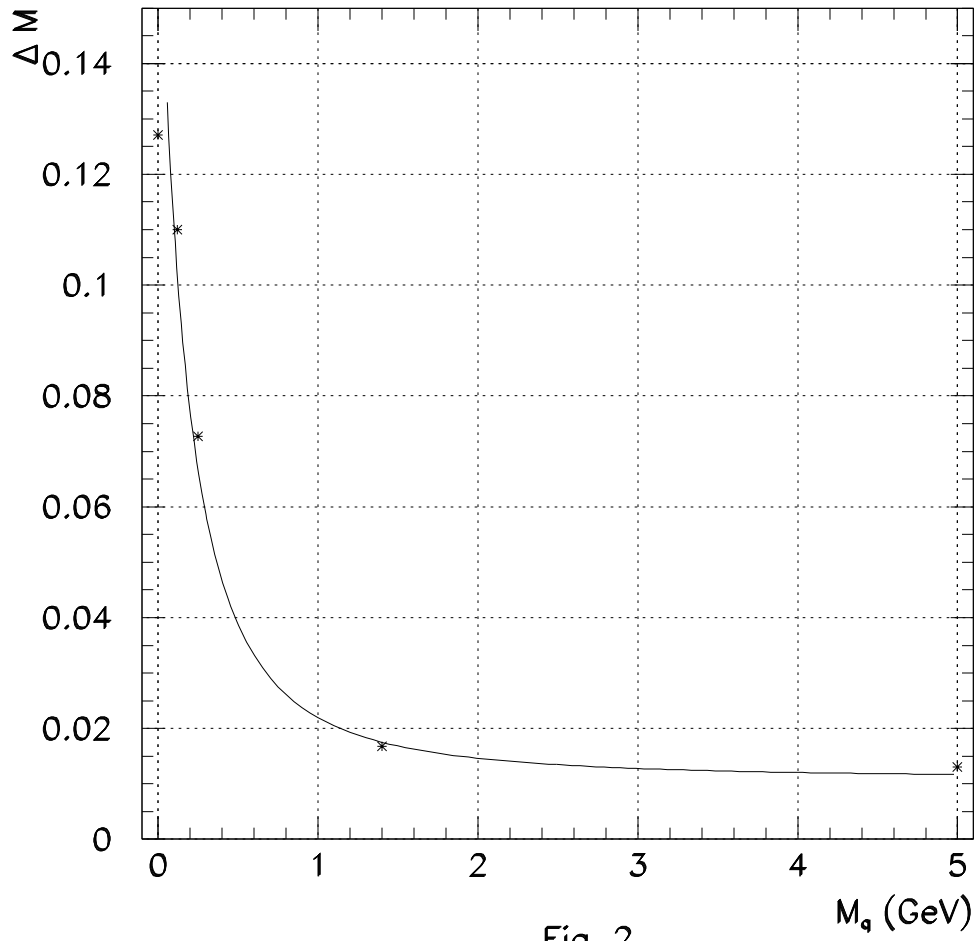


Fig. 2

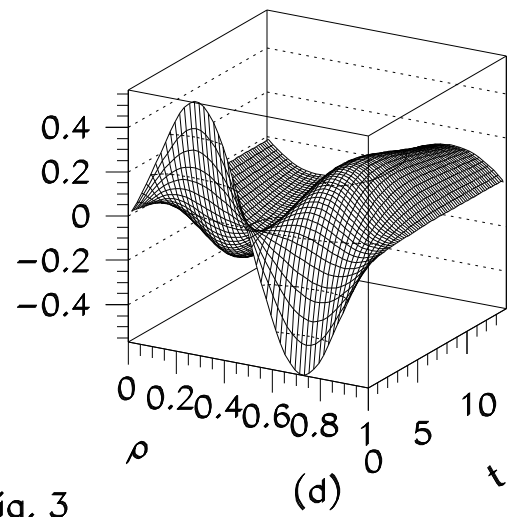
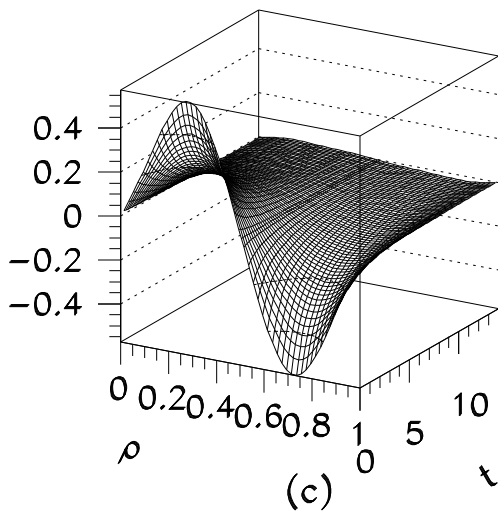
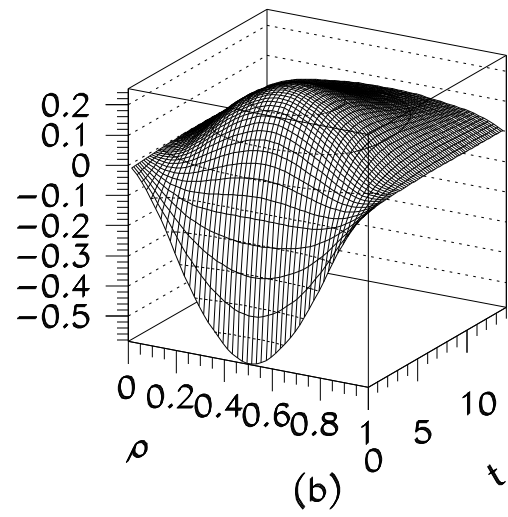
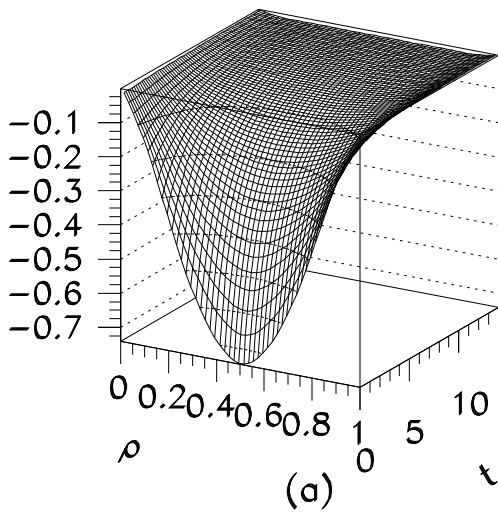


Fig. 3



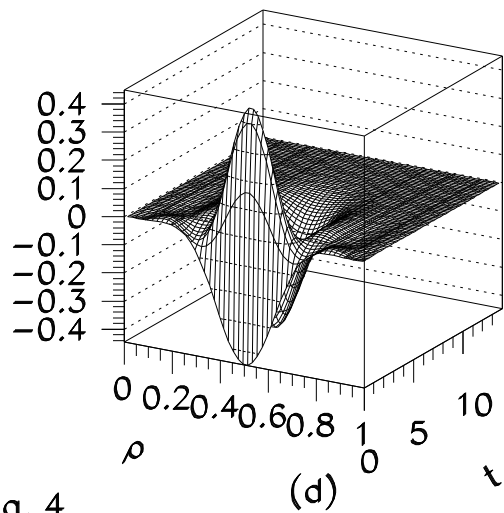
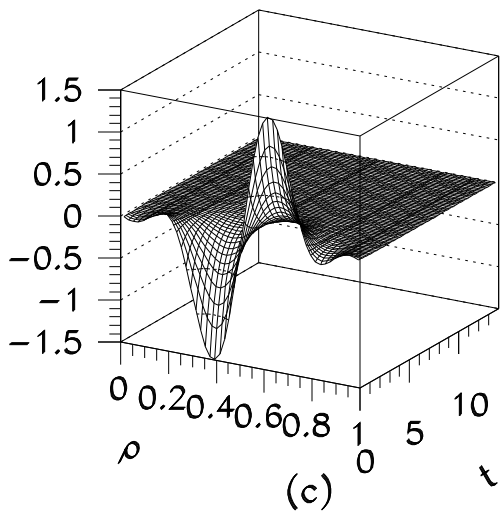
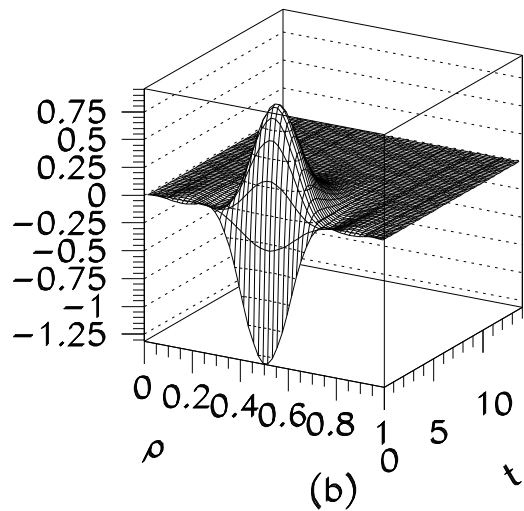
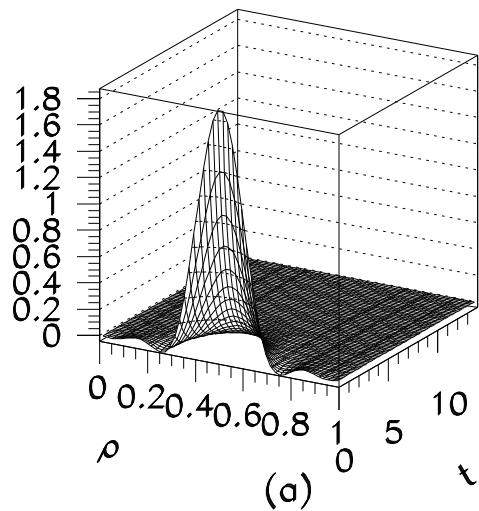


Fig. 4

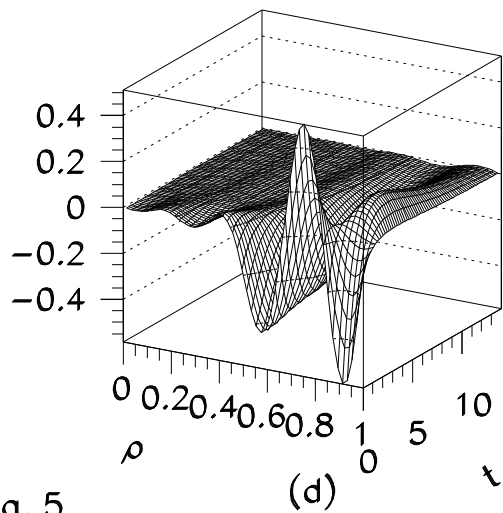
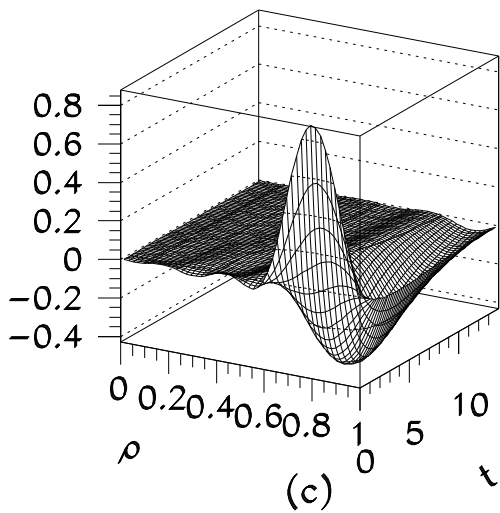
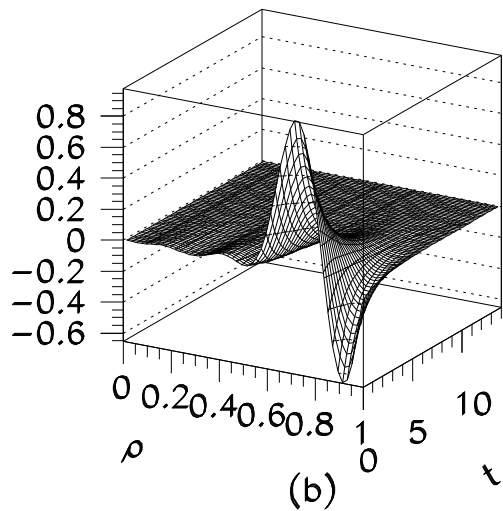
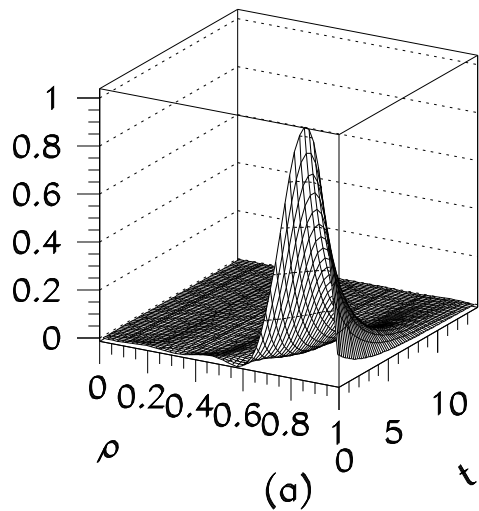
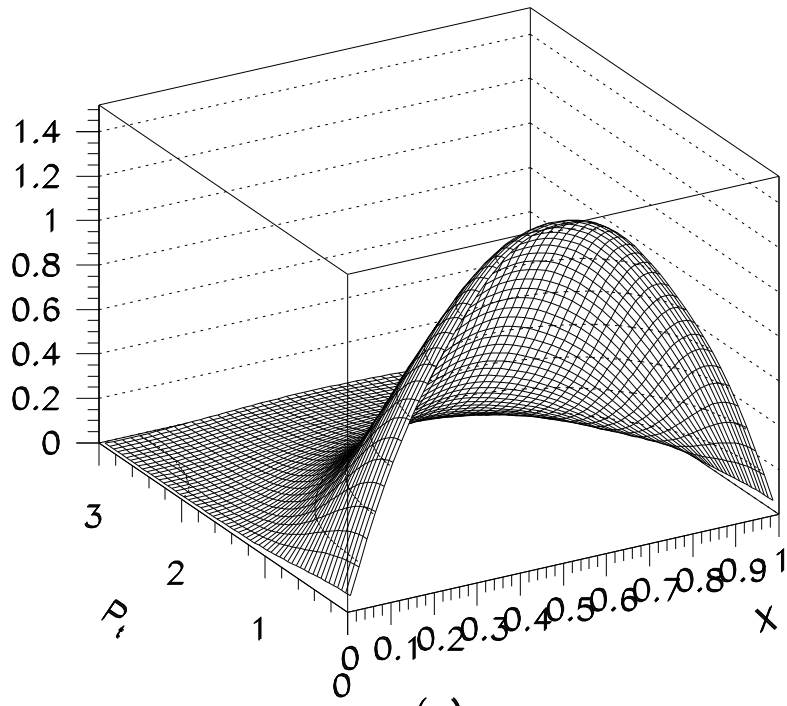
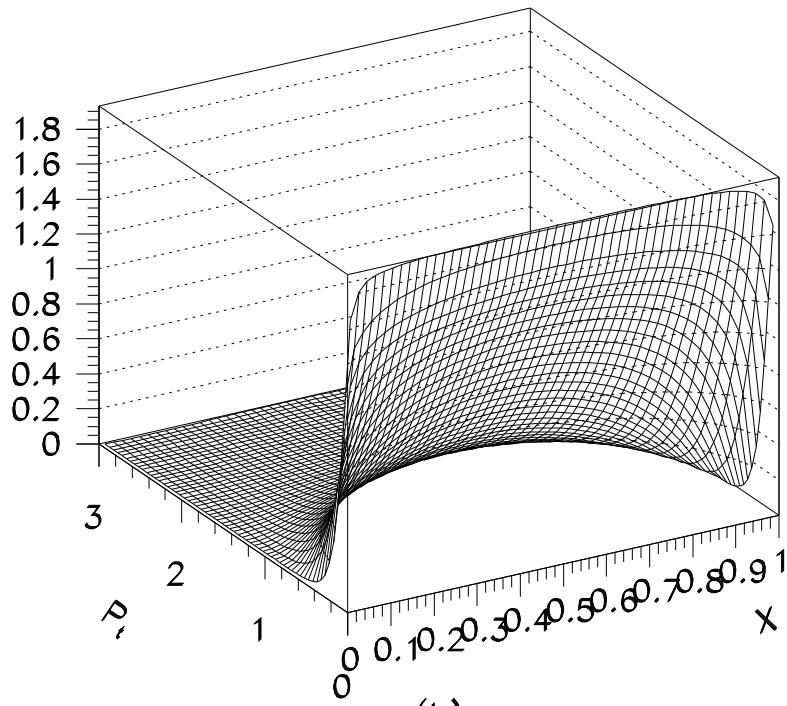


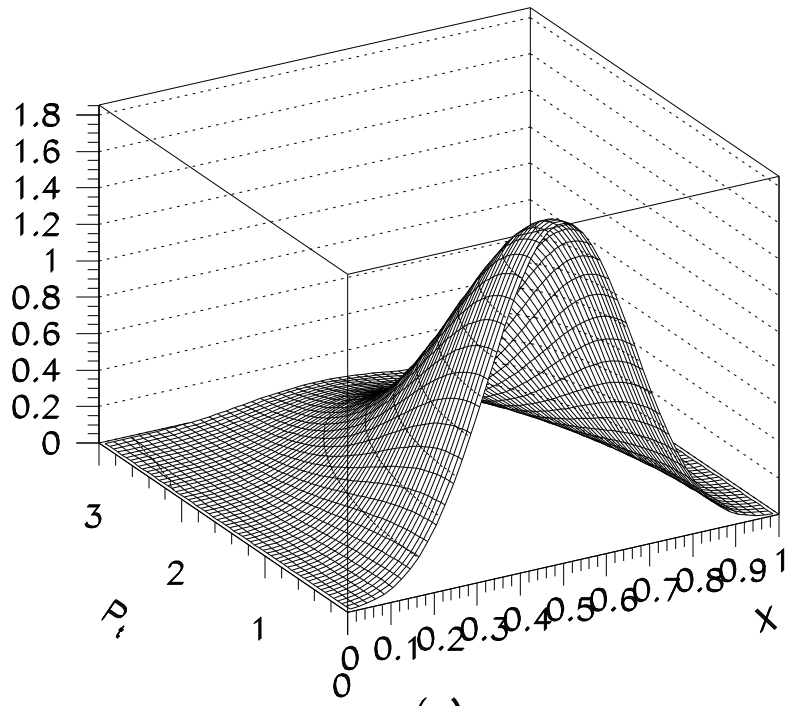
Fig. 5



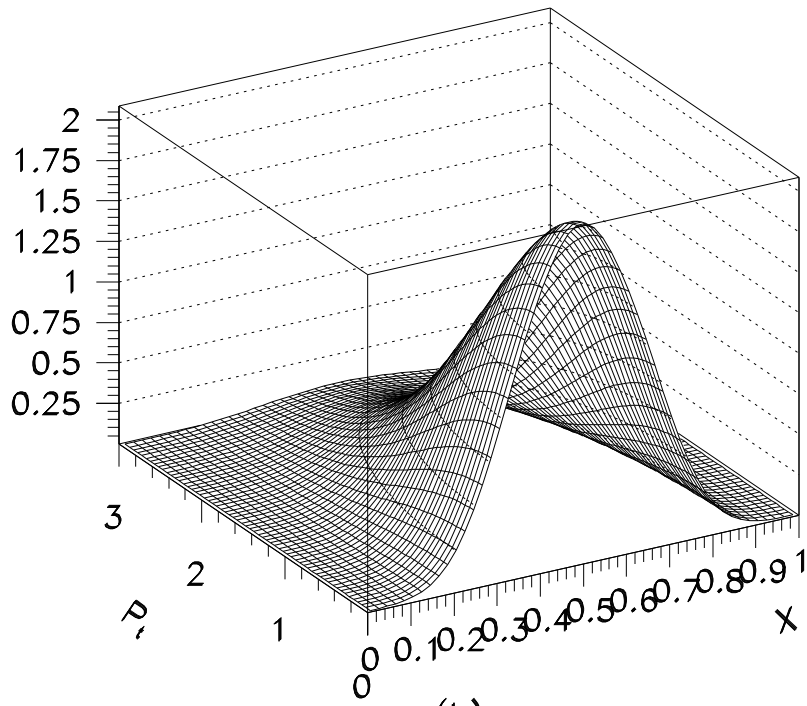
(a)



(b) Fig. 6



(a)



(b) Fig. 7

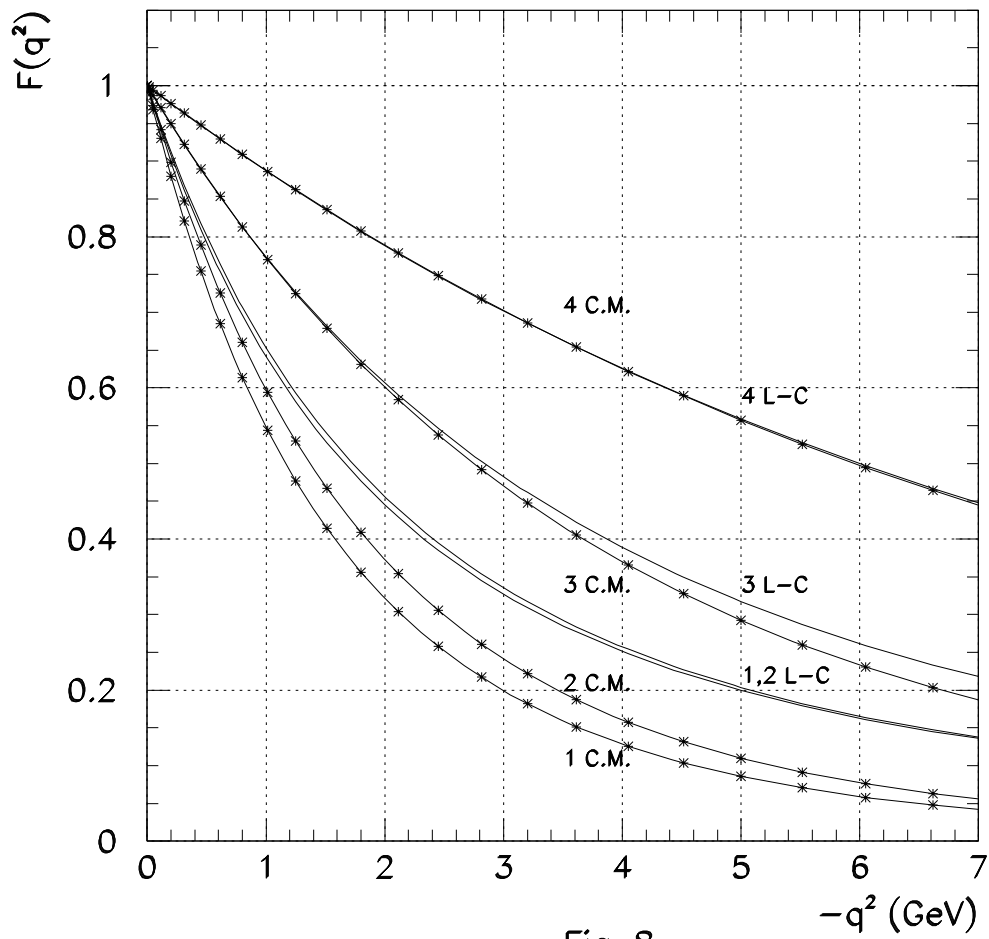


Fig. 8

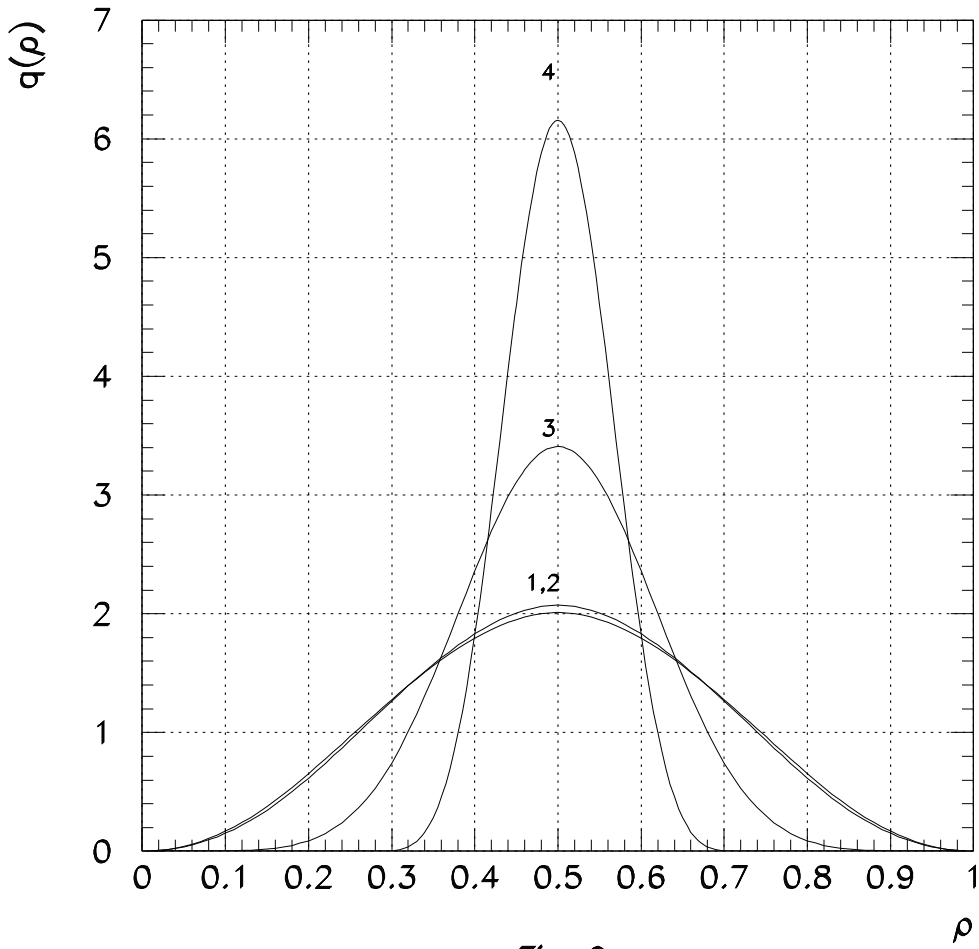


Fig. 9